Hindawi
Geofluids
Volume 2022, Article ID 1288463, 11 pages
https://doi.org/10.1155/2022/1288463

Research Article

Experimental Study on Mechanical Properties and Energy Evolution Law of Coal-Rock Composite Structure under Different Interface Connection Modes

Chenglin Tian,[1,2] Haitao Sun,[2,3] Linchao Dai,[2,3] Rifu Li,[2] Bo Wang,[2] Jie Cao,[2,3] Jun Wang,[1] and Qianting Hu[1,3]

[1]*State Key Laboratory of Mining Disaster Prevention and Control Co-founded by Shandong Province and the Ministry of Science and Technology, Shandong University of Science and Technology, Qingdao, Shandong 266590, China*
[2]*State Key Laboratory of the Gas Disaster Detecting, Preventing and Emergency Controlling, China Chongqing Research Institute of China Coal Technology and Engineering Group Crop., Chongqing 400037, China*
[3]*State Key Laboratory of Coal Mine Disaster Dynamics and Control, College of Resources and Security, Chongqing University, Chongqing 400044, China*

Correspondence should be addressed to Haitao Sun; dreamsht@163.com and Jun Wang; wangjunsdkjd@126.com

Received 17 November 2021; Accepted 25 January 2022; Published 17 March 2022

Academic Editor: Liang Xin

The stability of the coal-rock composite structure is of great significance to the safety production of deep mines, and the different interface connection modes of coal and rock have an important influence on its stability. Therefore, the following work was done in this article: Firstly, the mechanical structure model of coal-rock was established, and the influence of different interface connection modes on coal rock was analyzed. Secondly, the mechanical characteristics (plastic zone, stress, and displacement) of coal-rock composite structure under different interface connection modes were studied by numerical simulation, and the energy was quantitatively analyzed by FISH language in FLAC3D. The results were as follows: (1) The interface reduces the strength of rock and increases the strength of coal in the coal-rock composite structure. (2) In the loading process, the coal body is destroyed first and the destruction range increases gradually with the increase of stress. The failure mode is mainly a plastic shear failure, and the deformation of coal is much larger than that of rock in the composite structure. (3) The interface contact mode affects the mechanical behavior of coal and rock structure. The strong contact interface influences the strength, displacement, and energy accumulation of coal and rock structure, among which the influence on energy and displacement is greater, which is helpful to the improvement of strength. Therefore, it is suggested to adopt the strong contact interface in the study of coal and rock structure.

1. Introduction

Coal and coalbed methane mining are facing more severe challenges in deep mining, among which nonaqueous fracturing technologies have been gradually paid attention to as an environmentally friendly measure to increase permeability, and scholars have also done a lot of relevant studies [1–3]. However, the roof and floor also have an important impact on the mining of coal and coalbed methane. Practice shows that for soft broken low permeability coal seam, roof fracturing measures [4] can achieve better results, and the supercritical carbon dioxide antireflection measure [5] for coal seam can also achieve significant results. Roof and floor damage of different degrees have a significant impact on the increase of permeability of coal seams, but the dynamic disaster induced by the deep mining environment is also related to it. In deep mining environment, mine dynamic disasters gradually increase and are characterized by both rockburst and coal and gas outburst [6–9]. Compared with shallow mining, the different mechanical properties of coal and rock and the interaction between coal and rock in a deep mining environment must

be considered [10–12]. Because coal is in a certain surrounding rock environment, the mechanical characteristics of coal are different from that of single coal due to the difference in stiffness and interaction between coal and rock. Therefore, the study on the mechanical behavior of the coal-rock composite structure can better reflect the actual situation, which is of great significance to the efficient mining of coal and coalbed methane.

Researchers have carried out extensive research on the coal-rock composite structure. Liu et al. [13] carried out an experimental study on the damage and failure of layered composite rock, obtained the damage evolution process of the horizontal and vertical layered surrounding rock, and compared their differences. Lin et al. [14] studied the propagation and propagation of cracks in joint layered rock mass by uniaxial compression test. Huang et al. [15] studied the influence of loading rate on a coal-rock aggregate and found that the stiffness difference had a significant influence on the failure form and rockburst tendency of the aggregate. Zuo et al. studied the influence of combination mode [16], confining pressure, loading and unloading [17], and weak interlayer [18] on the mechanical characteristics and impact the liability of the composite body, analyzed the acoustic emission behavior during the loading process of the composite body, and found that the acoustic emission behavior is mainly affected by coal. Lu [19] and Wang et al. [20] studied the relationship between the bursting liability of coal-rock combination and the strength and thickness of coal and rock and tested their acoustic and electrical effects. Zhao et al. [21] experimentally studied the precursor information of deformation and failure of coal-rock mass. Chen et al. [22] studied the mechanical properties of coal-rock mass under the action of water rock. Levent Selcuk et al. [23] and Guo et al. [24] studied the influence of inclination angle on the strength and deformation failure of the composite body. Some researchers used uniaxial [25] and triaxial [26] compression tests to study the failure characteristics of coal-rock composite structures, the nonlinear evolution characteristics of energy, and the influence of cyclic loading and unloading [27–29]. Gong et al. [30] studied the influence of high loading rate on coal-rock assemblage. Liu et al. [31] studied the influence of rock strength on failure mode and mechanical properties of the composite body. Wu et al. [32] studied the mechanical characteristics and failure mechanism of anchoring coal-rock mass. Chen et al. [33] studied coal shale composites with high strength and low elastic modulus by uniaxial compression test. Chen et al. [34] used RFPA software to simulate the progressive failure characteristics of double-layer rocks and counted the number of microseismic events. Gao [35, 36] and Yang et al. [37] studied the failure characteristics and energy accumulation evolution process of coal-rock mass under dynamic and static loading through experiments and numerical simulation. Tan et al. [38] studied the influence of homogeneity on the rockburst tendency of coal and rock mass by particle flow simulation and analyzed acoustic emission characteristics. Ma et al. [39, 40] established a damage model considering coal thickness and studied the influence of coal-rock height ratio on the composite structure using particle flow. Du et al. [41] established a three-dimensional reconstruction model of coal-rock assemblage and studied the failure process and energy characteristics by numerical simulation. Wang et al. [42–44] studied the mechanical properties, permeability evolution, and acoustic emission characteristics of gas-bearing coal-rock assemblage under triaxial conditions. Lu et al. [45–47] studied the influence of mechanical properties, permeability evolution characteristics, and loading rate of lower-layer composite coal rock in a true triaxial environment.

In addition, Liu et al. [48] established the damage constitutive model of coal in coal and rock combination by carrying out experimental research. Zuo et al. [49] have established a prepeak nonlinear model of coal-rock mass based on axial crack evolution. Zuo et al. [50] and Song et al. [51], respectively, studied the postpeak failure behavior of coal-rock mass and established a nonlinear model. Petukhov et al. [52] established the failure theory based on the postpeak characteristics of rock and analyzed it from the perspective of energy. Qin et al. [53] studied the stability of the frame-column-roof system with catastrophe theory and established a damage evaluation model based on acoustic emission monitoring.

The above researches are mainly carried out from the angle of mechanical test and numerical simulation on the mechanical characteristics, energy dissipation, and damage evolution of coal and rock mass and have achieved fruitful results. However, the mechanical behavior and characterization of coal-rock composite structures are also related to coal-rock interaction.

Xie et al. [54] proposed and established a two-force model considering the interaction between the engineering body and geological body and verified its difference from the one-body two-media model by mechanical tests. Deng et al. [55] studied the failure process of rock structure by impact instability by numerical simulation. Zhao et al. [56, 57] established compression shear strength criterion considering interface effect. Zuo et al. [58] studied the mechanical characteristics of soft coal-rock combinations considering the interface effect. Yang et al. [59] used numerical simulation to study the acoustic emission energy evolution of progressive failure characteristics of the composite body under the influence of the interface effect. The above research shows that different connection modes of the coal-rock interface affect the interaction of coal, resulting in different deformation and failure characteristics and failure modes of the coal-rock structure.

To investigate the coal-rock interaction and its influence in the composite structure under different interface connection modes, this article firstly analyzed the influence of different interface contact modes on coal-rock interaction in composite structure theoretically. It then established the numerical calculation model of two different interface contact modes. Then numerical simulation is used to study the failure characteristics and energy accumulation evolution law of coal-rock composite structure under the

influence of different interface contact modes to clearly understand the mechanical response of the coal-rock composite structure under the influence of different interface contact modes.

2. Mechanical Structure Model of Coal-Rock Composite Structure

2.1. Influence of the Interface Connection Mode on the Composite Structure

2.1.1. Influence of Stress. The horizontal layered combined structure model (upper rock and lower coal) is constructed (Figure 1), where A represents rock and B represents coal. The elastic modulus of rock and coal are E_A, E_B; Poisson's ratios are μ_A, μ_B. The relationship between them meets the following requirements:

$$\begin{cases} E_A > EB, \\ \mu_A < \mu_B. \end{cases} \tag{1}$$

Assuming that there is no bonding force between A and B, then the horizontal strain of A and B satisfies the following equation:

$$\begin{cases} \varepsilon_{2A} = \varepsilon_{3A} = -\dfrac{\mu_A}{E_A}\sigma_1, \\ \varepsilon_{2B} = \varepsilon_{3B} = -\dfrac{\mu_B}{E_B}\sigma_1, \end{cases} \tag{2}$$

where ε_{2A} and ε_{2B} are the strains of A and B in the second direction, respectively, and ε_{3A} and ε_{3B} are the strains of A and B in the third direction, respectively.

Taking the microelement analysis at the interface, it is obvious that the coal and rock are constrained by each other at the interface due to different horizontal strains. At this point, the force of rock A at the interface changes from unidirectional compression to triaxial compression; the force of coal B at the interface changes from unidirectional compression to triaxial compression; the coal rock far away from the interface is still in unidirectional compression; then the binding force of rock A and B at the interface is as follows:

$$\begin{cases} \sigma_{2A} = \sigma_{1A} f_{2AB}, \\ \sigma_{3A} = \sigma_{1A} f_{3AB}, \\ \sigma_{2B} = \sigma_{1B} f_{2AB}, \\ \sigma_{3B} = \sigma_{1B} f_{3AB}. \end{cases} \tag{3}$$

Equation (3) satisfies the following:

$$\begin{cases} \sigma_{1A} = \sigma_{1B} = \sigma_1, \\ \sigma_{2A} = \sigma_{1B}, \\ \sigma_{3A} = \sigma_{3B}, \end{cases} \tag{4}$$

where σ_{2A} and σ_{2B}, respectively, represent the binding force of A and B in the second direction at the interface; σ_{3A} and σ_{3B}, respectively, represent the binding force of A and B in the third direction at the interface; σ_{1A} and σ_{2A}, respectively, represent the compressive stress of A and B in the first direction of the end face; and f_{2AB} and f_{3AB}, respectively, are the friction coefficients between A and B in the second and third directions.

2.1.2. Influence of Strength. The Mohr–Coulomb strength theory is applied to carry out specific analysis, wherein the linear expression of the Mohr strength curve is as follows:

$$\sigma_{1j} = \frac{1 + \sin\varphi}{1 - \sin\varphi}\sigma_{3j} + \frac{2c\cos\psi}{1 - \sin\varphi}. \tag{5}$$

Then,

$$\begin{cases} \sigma_{1j} = a\sigma_{3j} + R_c, \\ a = \dfrac{1 + \sin\varphi}{1 - \sin\varphi}, \\ R_c = \dfrac{2c\cos\psi}{1 - \sin\varphi}. \end{cases} \tag{6}$$

For rocks A and B in the combined structure, the equation can be obtained by the following analogy:

$$\sigma_{1j} = a_A\sigma_{3j} + R_{cA}, \tag{7}$$

$$\sigma_{1j} = a_B\sigma_{3j} + R_{cB}, \tag{8}$$

$$\begin{cases} a_A = \dfrac{1 + \sin\varphi_A}{1 - \sin\varphi_A}, \\ a_B = \dfrac{1 + \sin\varphi_B}{1 - \sin\varphi_B}, \end{cases} \tag{9}$$

where c and φ are, respectively, rock cohesion and internal friction angle; σ_j and τ_j are the normal stress and shear stress of the fracture surface, respectively; σ_{1j} and σ_{3j} are, respectively, the two ultimate principal stresses corresponding to rock in ultimate equilibrium; R_c is the uniaxial compressive strength of rock; and a is a parameter related to the angle of internal friction of rock.

For the stress analysis at the interface of A and B, when rock A at the interface is in the limit equilibrium state, it can be obtained according to equations (3) and (4):

$$\begin{cases} \sigma_{1j} = \sigma_{1A}, \\ \sigma_{3j} = \sigma_{3A} = -\sigma_{1A} f_{3AB}. \end{cases} \tag{10}$$

The axial ultimate strength of rock A at the interface can be obtained by formulas (10) and (7):

$$\sigma_{1Aj} = \frac{R_{cA}}{1 + a_A f_{3AB}}. \tag{11}$$

Similarly, if B is in the ultimate equilibrium state, it can be obtained according to equations (3) and (4):

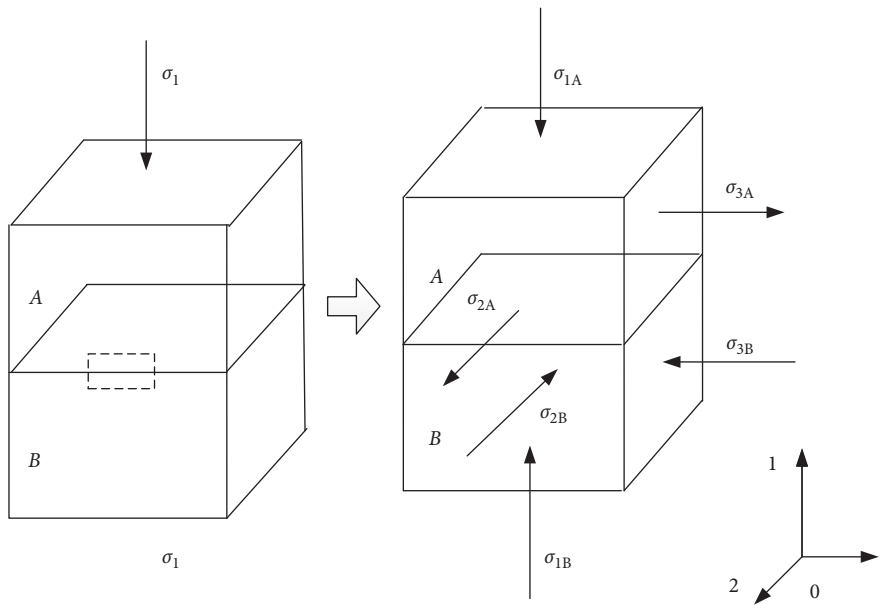

Figure 1: Force sketch map of the elastic body.

$$\begin{cases} \sigma_{1j} = \sigma_{1B}, \\ \sigma_{3j} = \sigma_{2A} = -\sigma_{1A} f_{2AB}. \end{cases} \tag{12}$$

The axial ultimate strength of rock B at the interface can be obtained by combining formulas (12) and (8):

$$\sigma_{1Bj} = \frac{R_{cB}}{1 - a_B f_{2AB}}. \tag{13}$$

The relationship between equations (11) and (13) are as follows:

$$\frac{R_{cA}}{1 + a_A f_{3AB}} < R_{cA}, \tag{14}$$

$$\frac{R_{cB}}{1 + a_B f_{2AB}} < R_{cB}. \tag{15}$$

According to equations (14) and (15), even though there is no cohesive force at the interface of coal and rock, the strength of coal and rock at the interface changes due to the existence of the interface. Specifically, the strength of the rock at the interface decreases, and the strength of coal increases.

2.2. Another Connection Mode: The Influence of Coal-Rock Interface with Cohesive Force on the Composite Structure

2.2.1. Influence of Stress. To distinguish interface binding force and end face stress, σ_i in Figure 1 is represented by σ_i'; according to Hooke's law, the strains of A and B in the second and third directions are as follows:

$$\begin{cases} \varepsilon_{2A}' = \dfrac{1}{E_A}\left[-\sigma_{1A}' - \mu_A\left(\sigma_{1A}' - \sigma_{3A}'\right)\right], \\ \varepsilon_{2B}' = \dfrac{1}{E_B}\left[-\sigma_{1B}' - \mu_B\left(\sigma_{1B}' - \sigma_{3B}'\right)\right], \end{cases} \tag{16}$$

$$\begin{cases} \varepsilon_{3A}' = \dfrac{1}{E_A}\left[-\sigma_{3A}' - \mu_A\left(\sigma_{1A}' - \sigma_{2A}'\right)\right], \\ \varepsilon_{3B}' = \dfrac{1}{E_B}\left[-\sigma_{3B}' - \mu_B\left(\sigma_{1B}' - \sigma_{2B}'\right)\right]. \end{cases} \tag{17}$$

The stress-strain satisfaction relationship of the micro-element is as follows:

$$\begin{cases} \sigma_{2A}' = \varepsilon_{2B}' = \varepsilon_2', \\ \sigma_{3A}' = \varepsilon_{3B}' = \varepsilon_3', \\ \varepsilon_2' = \varepsilon_3', \end{cases} \tag{18}$$

$$\begin{cases} \sigma_{1A}' = \sigma_{1B}' = \sigma_1, \\ \sigma_{2A}' = \sigma_{2B}' = \sigma_2', \\ \sigma_{3A}' = \sigma_{3B}' = \sigma_3', \\ \sigma_2' = \sigma_3'. \end{cases} \tag{19}$$

According to equations (15)–(18), it can be solved as follows:

$$\begin{cases} \sigma_{2A}' = \sigma_{2B}' = \sigma_{3A}' = \sigma_{3B}' = \sigma_2' = \sigma_3' \\ = \dfrac{E_A\mu_B - E_B\mu_A}{E_A\left(1 - \mu_B\right) + E_B\left(1 - \mu_A\right)} \cdot \sigma_1, \\ \sigma_{1A}' = \sigma_{1B}' = \sigma_1. \end{cases} \tag{20}$$

The strength of coal and rock far from the interface is limited by horizontal binding force and can be ignored; that is, the one-way stress that the strength of rock far from the interface is still affected by σ_1:

$$\begin{cases} \sigma_{1A} = \sigma_{1B} = \sigma_1, \\ \sigma_{2A} = \sigma_{2B} = 0, \\ \sigma_{3A} = \sigma_{3B} = 0. \end{cases} \tag{21}$$

2.2.2. Influence of Strength. Assuming that the strengths of A and B still meet equations (7) and (8), when A is in the ultimate equilibrium state at the interface of A and B, the ultimate stress of A can be obtained according to equation (20):

$$\begin{cases} \sigma_{1j} = \sigma_{1A}', \\ \sigma_{3j} = \sigma_{1A}'\gamma_{AB}. \end{cases} \tag{22}$$

Similarly, when B is in the ultimate equilibrium state, the ultimate stress of B can be obtained:

$$\begin{cases} \sigma_{1j} = \sigma_{1B}', \\ \sigma_{3j} = \sigma_{1B}'\gamma_{AB}. \end{cases} \tag{23}$$

$$\gamma_{AB} = \frac{E_A\mu_A - E_B\mu_A}{E_A(1-\mu_B) + E_B(1-\mu_A)} > 0, \tag{24}$$

$$\sigma_{1A}' > 0, \tag{25}$$

$$\sigma_{1B}' > 0, \tag{26}$$

According to (7) and (22) and equations (8) and (23), the axial ultimate strengths of A and B are as follows:

$$\sigma_{1A}' = \frac{R_{cA}}{1 + a_A\gamma_{AB}}, \tag{27}$$

$$\sigma_{1B}' = \frac{R_{cB}}{1 - a_A\gamma_{AB}}. \tag{28}$$

The relationship between equations (27) and (28) are as follows:

$$\frac{R_{cA}}{1 + a_A\gamma_{AB}} < R_{cA}, \tag{29}$$

$$\frac{R_{cB}}{1 + a_B\gamma_{AB}} < R_{cB}. \tag{30}$$

According to equations (29) and (30), when there is the cohesive force at the interface of coal and rock, the strength of coal and rock at the interface is also affected, as shown in the following: the strength of the rock at the interface decreases and the strength of coal increases.

2.3. Comparison of the Influence of Different Interface Connection Modes on Composite Structure. By comparing equations (11) and (13) and (27) and (28), respectively, it is found that the two sets of equations are only differences between f_{AB} and γ_{AB}, because $\gamma_{AB} > f_{AB}$; the following can be known:

$$R_{cA} > \frac{R_{cA}}{1 + a_A f_{3AB}} > \frac{R_{cA}}{1 + a_A\gamma_{AB}}, \tag{31}$$

$$R_{cA} > \sigma_{1Aj} > \sigma_{1Aj}', \tag{32}$$

$$\frac{R_{cB}}{1 - a_B\gamma_{AB}} > \frac{R_{cB}}{1 - a_B f_{2AB}} > R_{cB}, \tag{33}$$

$$\sigma_{1Bj} > \sigma_{1Aj}' > R_{cB}. \tag{34}$$

According to equations (31)–(34), it can be seen that the cohesive force between the interface has different influences on the strength of coal and rock. With the increase of the cohesive force between the interface, the strength of the rock at the interface is reduced and the strength of coal is increased.

3. Numerical Simulation

To facilitate the numerical simulation, the following assumptions are made: (1) the mechanical properties of coal rock are not very different, which can be expressed as follows: The strength of coal failure can also cause a certain amount of energy accumulation in roof rock, allowing partial failure of rock but still maintaining sufficient bearing capacity. (2) The coal-rock interface is divided into strong contact and weak contact according to the contact surface treatment in the simulation. The strong contact can ensure the continuous transmission of stress displacement. In the case of strong contact, the attached face all command is directly used to connect the coal-rock grid. (3) The weak contact is mainly realized by changing the mechanical parameters of the contact surface.

3.1. Simulation Scheme. FLAC3D software was used to establish the numerical calculation model of loading of coal-rock composite structure uniaxial cylindrical specimen. The total height of the model is 100 mm, the diameter of the cylindrical specimen is 50 mm, the height ratio of coal to rock is 1 : 1, the combination of coal and rock is a horizontal combination, the total number of model elements is 51200, and the number of nodes is 52833. The Mohr model is used in the constitutive model. The initial model is shown in Figure 2. Mechanical parameters of coal and rock are shown in Table 1.

Three different stages are set up in the loading process, which are prepeak elastic section, peak point, and post-peak failure, respectively. The plastic zone, stress, strength, displacement, and energy distribution of corresponding stages were extracted and compared. The mechanical parameters of the contact surface are shown in Table 2.

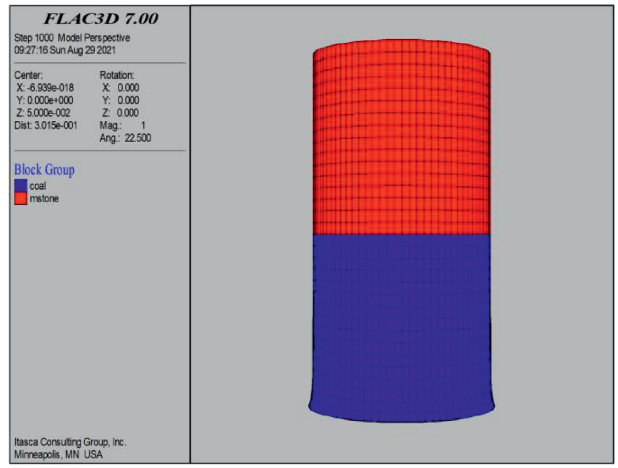

Figure 2: The initial model.

Table 1: The thicknesses and parameters of the coal seams and rock strata.

Rock category	Thickness (mm)	Density (g/cm^3)	Bulk modulus (GPa)	Shear modulus (GPa)	Cohesion (MPa)	Frictional angle (°)	Tension (MPa)
Sandy mudstone	50	2455.45	3.48	2.26	5.51	38	4.29
Coal	50	1625.75	1.52	0.81	2.10	30	1.25

Table 2: The parameters of the interface.

Category	Shear stiffness (GPa)	Normal stiffness (GPa)	Cohesion (MPa)	Frictional angle (°)	Tension (MPa)
Weak interface	3.5*e*2	2.6*e*2	2.8	19.0	2.2

3.2. Numerical Simulation Results and Analysis

3.2.1. Distribution Characteristics and Evolution Law of Plastic Zone. Figures 3(a)–3(c) show, respectively, for the coal-rock interface weak contact of the plastic zone distribution and Figures 3(d)–3(f), respectively, the coal-rock interface strong contact of the plastic zone distribution. Figures 3(a) and 3(d), Figures 3(b) and 3(e), and Figures 3(c) and 3(f) show the prepeak, peak, and postpeak distribution of the plastic zone, respectively.

According to Figures 3(a) and 3(b), the plastic zone at the elastic segment and peak point are almost unchanged during weak contact, and the plastic zone may be formed at the initial stage of loading. The plastic zone does not expand during loading to the peak point, and the plastic damage is limited to the lower coal body. According to Figures 3(d) and 3(e), the plastic zone at the elastic segment and peak value are significantly different in strong contact, and the plastic zone at the peak value is significantly larger than that at weak contact.

According to Figures 3(c) and 3(f), the postpeak energy release of coal accelerates the expansion of the plastic zone, resulting in integral failure of the coal body and tensile failure of the rock near the interface corner to a certain extent. The rock part is relatively intact, and the rock near the interface corner after the peak also produces tensile failure to a certain extent, which is more serious than the weak contact.

3.2.2. Distribution Characteristics and Evolution Law of Stress. Figures 4(a)–4(c) show, respectively, the coal-rock interface weak contact of the vertical stress distribution, and Figures 4(d)–4(f), respectively, the coal-rock interface strong contact of the vertical stress distribution. Figures 4(a) and 4(d), Figures 4(b) and 4(e), and Figures 4(c) and 4(f) show the prepeak, peak, and postpeak distribution of the vertical stress, respectively.

According to Figures 4(a) and 4(b), the distribution of stress at the peak of weak contact is generally similar to that in the elastic segment, and the stress at the interface edge of coal-rock and in the middle and lower part of coal increases relatively, but the increase is limited. The overall distribution of stress in the model is still relatively uniform. The stress distribution under a strong contact surface is quite different. In the coal body part of the model, low-stress areas with inverted V-shaped distribution appeared (Figure 4(d)), indicating that these areas have produced damage and failure of varying degrees and reduced bearing capacity. At the same time, there is a certain degree of stress concentration in the middle of the coal body, but the area is very small. In the case of strong interface contact, the constraint effect on coal near the interface is stronger, which

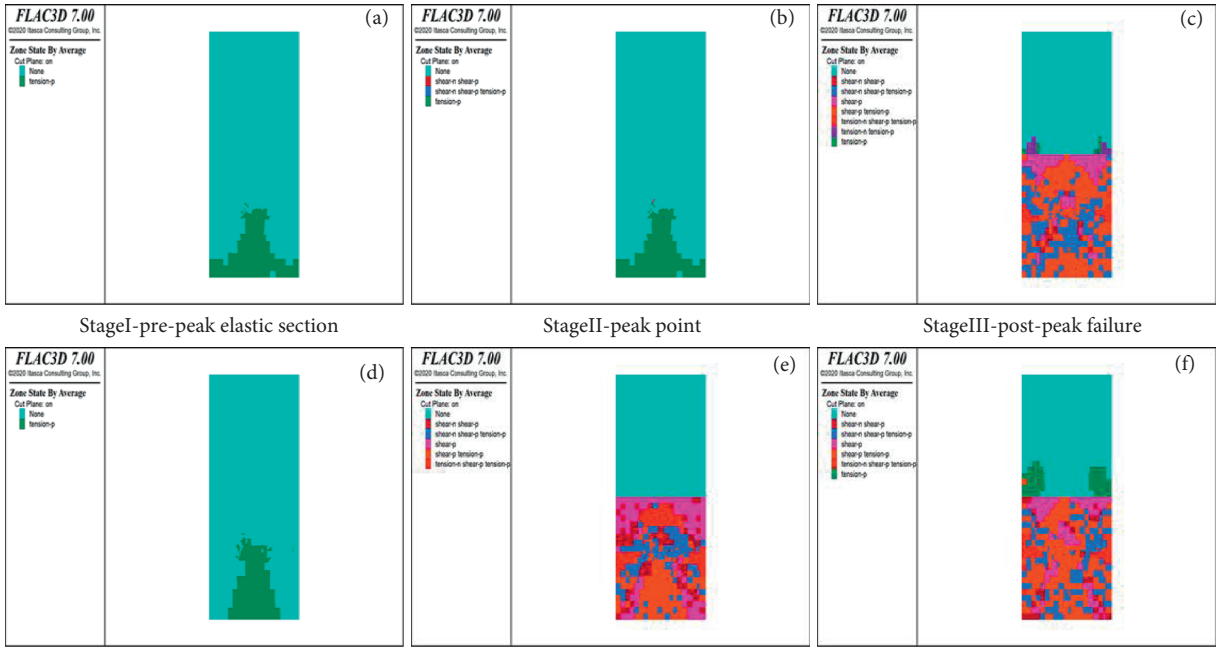

Figure 3: Distribution of the plastic zone under different conditions.

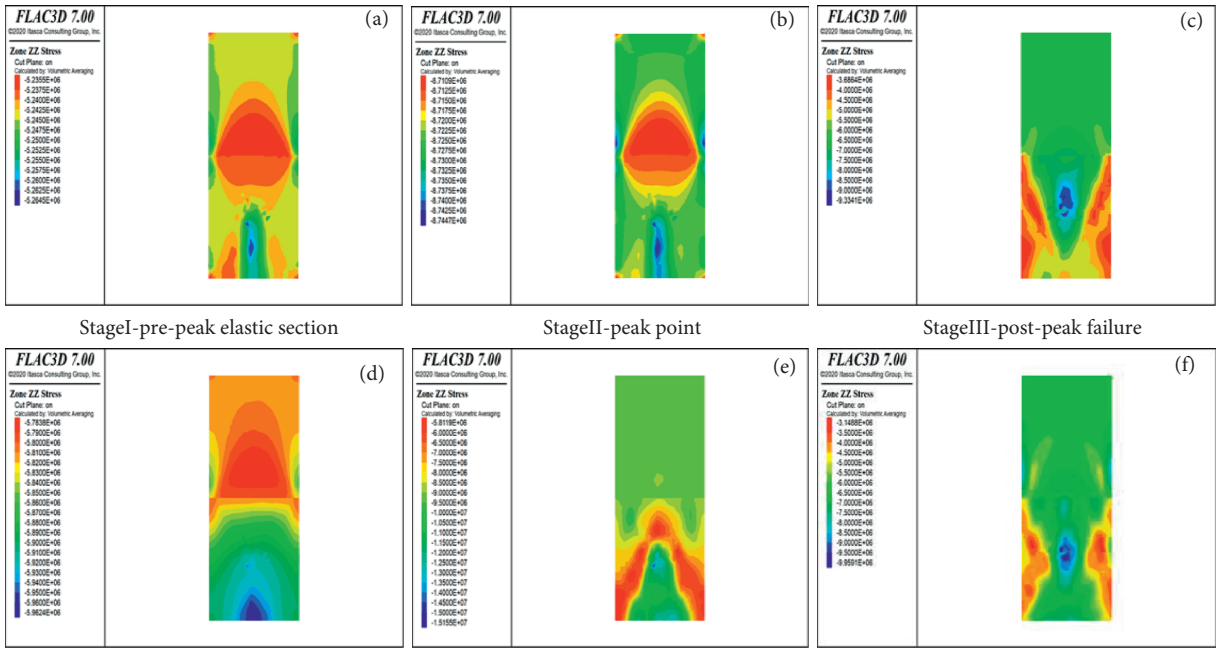

Figure 4: Vertical stress distribution under different conditions.

improves the bearing capacity of coal to a certain extent. The energy release under the two contact modes is mainly from coal.

3.2.3. Distribution Characteristics and Evolution Law of Displacement. Figures 5(a)–5(c) show, respectively, the coal-rock interface weak contact of the displacement distribution, and Figures 5(d)–5(f), respectively, the coal-rock interface strong contact of the displacement distribution. Figures 5(a) and 5(d), Figures 5(b) and 5(e), and Figures 5(c) and 5(f) show the prepeak, peak, and postpeak distribution of the displacement, respectively.

According to Figures 5(a), 5(b), 5(d), and 5(e), it can be seen that the displacement changes of an elastic segment and peak segment are similar regardless of weak contact or strong contact, and the displacement gradually increases with the increase of load. By comparing Figures 5(b), 5(e), 5(c), and 5(d), it can be seen that the deformation at the peak and after the peak of the composite is larger than that of the strong contact at the coal-rock interface under weak contact.

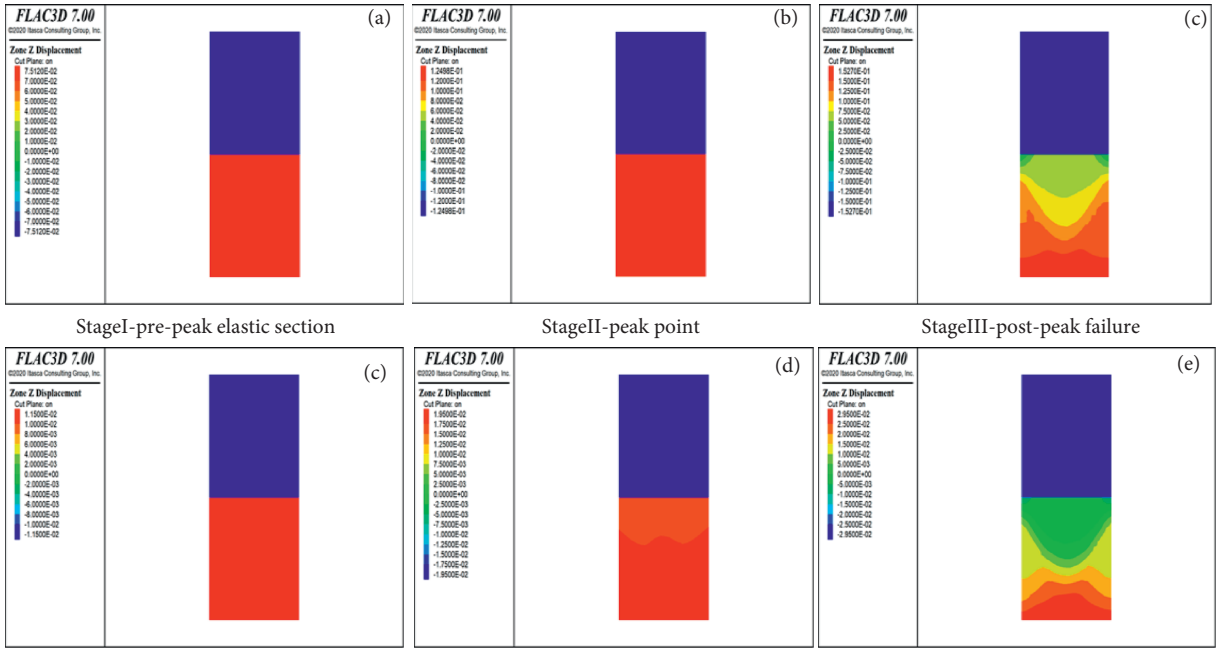

Figure 5: Displacement distribution under different conditions.

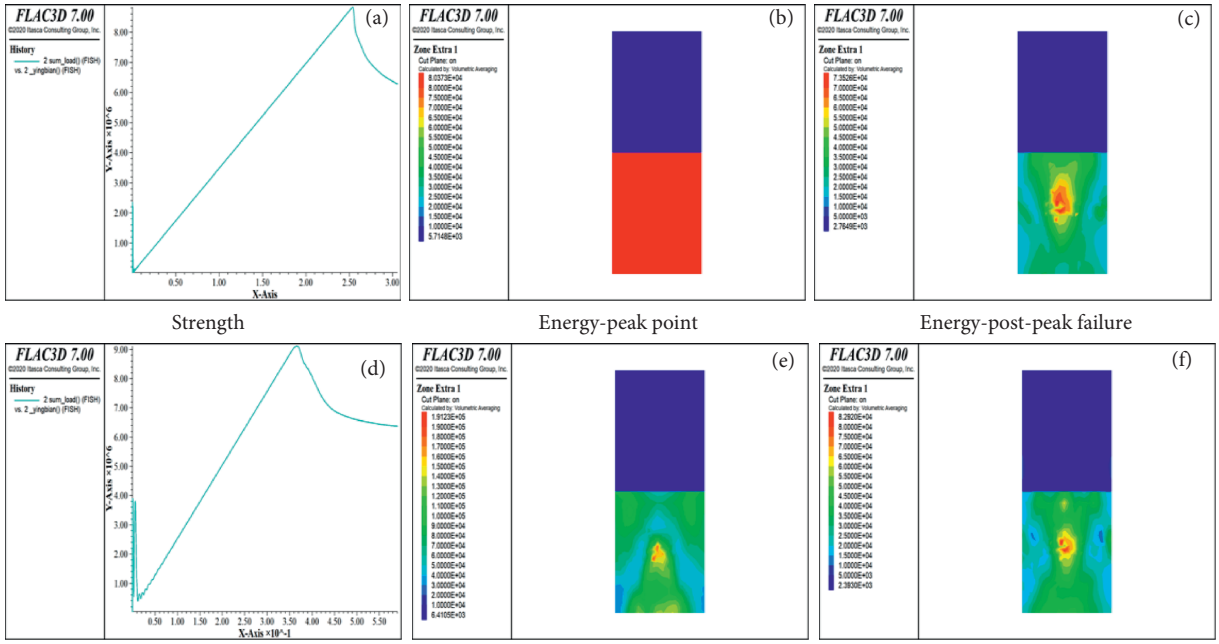

Figure 6: Comparison of strength and elastic energy.

This indicates that weak contact can cause larger deformation of the coal-rock structure.

3.2.4. Distribution Characteristics and Evolution Law of Energy. In order to further analyze the evolution process of coal and rock energy in the loading process, fish language in FLAC3D software was applied to calculate the energy of composite structure at different stress stages. The energy distribution of rock and coal in the combined structure is extracted, respectively, and the overall strength of the combined structure is obtained.

Figures 6(a) and 6(d) show the peak strength of weak contact and strong contact at the coal-rock interface, respectively. It can be seen that the strength of coal and rock mass in strong contact is 9.2 MPa, which is larger than

8.8 MPa in weak contact, and the peak strain decreases. This may be the result of the strong contact between coal and rock, which makes the coal-rock interaction more obvious.

Figures 6(b) and 6(e) show the energy distribution of coal and rock at the peak point, and Figures 6(c) and 6(e) show the postpeak energy distribution. The energy accumulation of coal and rock is also different in strong contact. Specifically, under a strong contact interface, the overall energy of the system is higher. In strong contact, the maximum energy in coal is 191.2 kJ and the minimum energy in rock is 6.41 kJ. In the case of a weak contact surface, the maximum energy in coal is 80.3 kJ, and the minimum energy in rock is 5.71 kJ. There is a large difference between the two. Therefore, it can be seen that the interface contact degree has an impact on the strength and energy accumulation of coal and rock, and the impact on energy is the most serious. After the peak, with the release of energy, the accumulated elastic energy of rock gradually decreases and eventually becomes stable.

The strong contact interface has a stronger constraining effect on coal and rock, which improves the resistance of coal to deformation and damage. The influence of interface contact mode should be fully considered in the study of coal-rock structures.

4. Discussion

(1) Considering the real engineering environment, coal seam and rock are stratified rock masses. The influence of interface contact mode is the influence of the degree of cementation between the coal seam and rock. The strength of the interlayer cementation is equal to the strength of the interface contact mode studied in this article.

(2) When the strength difference between the two layers is large, the influence of the interface is relatively limited. This is mainly because the strength of the unstable coal is not enough to cause enough deformation of the rock, resulting in limited energy accumulation of the rock itself. At this time, the combined structure disaster instability is similar to that of a single coal body, and the coal-rock interaction is not obvious. When both rocks are of high strength and the strength difference is small, the degree of cementation between the rocks is usually better. This makes the composite structure have strong shear resistance, and it is usually accompanied by a strong dynamic effect during the disaster instability, and the interaction between coal and rock is obvious.

(3) The interface connection mode is also one of the factors affecting the coal-rock interaction. It involves stress transfer and deformation coordination, which then affects the failure process and failure form of structures. In addition, it may cause changes in the strength of composite structures. Therefore, it is more helpful for engineering disaster prevention to clarify the interface connection mode.

5. Conclusion

By taking the coal-rock composite structure as a research object, based on theoretical analysis and numerical simulations, the concrete influence of interface connection mode on the coal-rock composite structure was studied; the stress, displacement, plastic zone and energy distribution, and evolution of composite structure under different contact modes were analyzed by numerical simulation. The main conclusions were as follows:

(1) The interface influences the coal-rock composite structure, which is shown as follows: the interface reduces the strength of rock and increases the strength of coal in the composite structure. The interface connects coal and rock as a whole to resist external loads. The failure of coal provides favorable conditions for the release of rock elastic energy, which ultimately leads to the instability of the composite structure.

(2) In the process of loading, the coal body is destroyed first, and the range of failure increases gradually with the increase of stress. The failure direction extends from the bottom to the coal-rock interface, and the failure form is mainly plastic shear failure. At the coal-rock interface, tensile failure occurs to a certain extent, and rock deformation is relatively uniform and small. The deformation of coal increases gradually from top to bottom, and the deformation is larger than that of rock.

(3) The interface contact mode affects the mechanical behavior of coal and rock structure. The strong contact interface influences the strength, displacement, and energy accumulation of coal and rock structures, among which the influence on the energy and displacement is great, which is helpful to the improvement of strength, but it is not obvious on the whole. Therefore, it is suggested to adopt the strong contact interface in the study of coal and rock structure.

Data Availability

The data used to support the findings of this study are included in the article.

Conflicts of Interest

The authors declare there are no conflicts of interest regarding the publication of this article.

Acknowledgments

This work was financially supported by the National Natural Science Foundation of China (51874348, 51574280 and 52104239), Chongqing Science Fund for Distinguished Young Scholars (cstc2019jcyjjqX0019), and Science and Technology Innovation and Entrepreneurship Fund of

China Coal Technology Engineering Group (2019-TD-QN040).

References

[1] F. Yan, J. Xu, S. Peng et al., "Breakdown process and fragmentation characteristics of anthracite subjected to high-voltage electrical pulses treatment," *Fuel*, vol. 275, Article ID 117926, 2020.

[2] F. Yan, J. Xu, B. Lin, S. Peng, Q. Zou, and X. Zhang, "Effect of moisture content on structural evolution characteristics of bituminous coal subjected to high-voltage electrical pulses," *Fuel*, vol. 241, pp. 571–578, 2019.

[3] F. Yan, J. Xu, B. Lin, S. Peng, Q. Zou, and X. Zhang, "Changes in pore structure and permeability of anthracite coal before and after high-voltage electrical pulses treatment," *Powder Technology*, vol. 343, pp. 560–567, 2019.

[4] H. Li, W. Liang, and G. Li, "The ductile failure-seepage coupling constitutive equations of broken soft coal and its and its verification in indirect fracturing engineering," *Journal of China Coal Society*, vol. 46, no. 3, pp. 924–936, 2021.

[5] X. Yang, G. Wen, H. Sun et al., "Environmentally friendly techniques for high gas content thick coal seam stimulation—multi-discharge CO_2 fracturing system," *Journal of Natural Gas Science and Engineering*, vol. 61, pp. 71–82, 2019.

[6] K. Wang and F. Du, "Coal-gas compound dynamic disasters in China: a review," *Process Safety and Environmental Protection*, vol. 133, pp. 1–17, 2020.

[7] L. Yuan, Y. D. Jiang, and X. Q. He, "Research progress of precise risk accurate identification and monitoring early warning on typical dynamic disasters in coal mine," *Journal of China Coal Society*, vol. 43, no. 2, pp. 306–318, 2018.

[8] J. Wang, D. B. Apel, Y. Pu, R. Hall, C. Wei, and M. Sepehri, "Numerical modeling for rockbursts: a state-of-the-art review," *Journal of Rock Mechanics and Geotechnical Engineering*, vol. 13, no. 2, pp. 457–478, 2021.

[9] J. Wang, D. B. Apel, A. Dyczko et al., "Investigation of the rockburst mechanism of driving roadways in close-distance coal seam mining using numerical modeling method," *Mining, Metallurgy & Exploration*, vol. 38, no. 5, pp. 1899–1921, 2021.

[10] J. Lu, G. Yin, H. Gao et al., "True triaxial experimental study of disturbed compound dynamic disaster in deep underground coal mine," *Rock Mechanics and Rock Engineering*, vol. 53, no. 5, pp. 2347–2364, 2020.

[11] Y. S. Pan, "Integrated study on compound dynamic disaster of coal-gas outburst and rockburst," *Journal of China Coal Society*, vol. 41, no. 1, pp. 105–112, 2016.

[12] L. Y. Zhu, Y. S. Pan, and Z. H. Li, "Mechanisms of rock burst and outburst compound disaster in deep mine," *Journal of China Coal Society*, vol. 43, no. 11, pp. 3042–3050, 2018.

[13] L. Liu, X. Qiu, M. Huang, and Z. Yan, "Experimental study on damage and failure of layered composite rock," *Journal of Chongqing University (Natural Science)*, vol. 22, no. 4, pp. 28–33, 1999.

[14] Q. Lin, P. Cao, G. Wen, J. Meng, R. Cao, and Z. Zhao, "Crack coalescence in rock-like specimens with two dissimilar layers and pre-existing double parallel joints under uniaxial compression," *International Journal of Rock Mechanics and Mining Sciences*, vol. 139, Article ID 104621, 2021.

[15] B. Huang and J. Liu, "The effect of loading rate on the behavior of samples composed of coal and rock," *International Journal of Rock Mechanics and Mining Sciences*, vol. 61, pp. 23–30, 2013.

[16] J. P. Zuo, Y. Chen, and F. Cui, "Differences in mechanical properties and impact tendency of different coal and rock combinations," *Journal of China University of Mining and Technology*, vol. 47, no. 1, pp. 81–87, 2018.

[17] J. P. Zuo, H. P. Xie, B. B. Meng, and J. F. Liu, "Experimental research on loading-unloading behavior of coal-rock combination bodies at different stress levels," *Rock and Soil Mechanics*, vol. 32, no. 5, pp. 1287–1296, 2011.

[18] J. Zuo, Z. Wang, H. Zhou, J. Pei, and J. Liu, "Failure behavior of a rock-coal-rock combined body with a weak coal interlayer," *International Journal of Mining Science and Technology*, vol. 23, no. 6, pp. 907–912, 2013.

[19] C. P. Lu, L. M. Dou, and X. R. Wu, "Experimental research on rules of rockburst tendency evolution and acoustic electromagnetic effects of compound coal-rock samples," *Chinese Journal of Rock Mechanics and Engineering*, vol. 26, no. 12, pp. 2549–2555, 2007.

[20] X. N. Wang, C. P. Lu, and J. H. Xue, "Experimental research on rules of acoustic emission and microseismic effects of burst failure of compound coal-rock samples," *Rock and Soil Mechanics*, vol. 34, no. 9, pp. 2569–2575, 2013.

[21] Y. X. Zhao, Y. D. Jiang, J. Zhu, and G. Z. Sun, "Experimental study on precursory information of deformations of coal rock composite samples before failure," *Chinese Journal of Rock Mechanics and Engineering*, vol. 27, no. 2, pp. 339–346, 2008.

[22] G. B. Chen, J. W. Zhang, and T. Li, "Study on the timeliness of damage and deterioration of mechanical properties of coal-rock combined body under water-rock interaction," *Journal of China Coal Society*, 2021.

[23] L. Selçuk and D. Aşma, "Experimental investigation of the Rock–Concrete bi materials influence of inclined interface on strength and failure behavior," *International Journal of Rock Mechanics and Mining Sciences*, vol. 123, pp. 1–11, 2019.

[24] D. M. Guo, J. P. Zuo, Y. Zhang, and R. S. Yang, "Research on strength and failure mechanism of deep coal-rock combination bodies of different inclined angles," *Rock and Soil Mechanics*, vol. 32, pp. 1332–1339, 2011.

[25] Y. Chen, J. Zuo, D. Liu, and Z. Wang, "Deformation failure characteristics of coal-rock combined body under uniaxial compression: experimental and numerical investigations," *Bulletin of Engineering Geology and the Environment*, vol. 78, no. 5, pp. 3449–3464, 2019.

[26] Y. L. Chen, J. P. Zuo, and D. J. Liu, "Experimental and numerical study of coal-rock bimaterial composite bodies under triaxial compression," *International Journal of Coal Science & Technology*, vol. 5, pp. 1–12, 2021.

[27] Z. H. Zhu, T. Feng, and F. Q. Gong, "Experimental research of mechanical properties on grading cycle loading–unloading behavior of coal–rock combination bodies at different stress levels," *Journal of Central South University*, vol. 47, pp. 2469–2475, 2016.

[28] S. Song, X. Liu, Y. Tan, D. Fan, Q. Ma, and H. Wang, "Study on failure modes and energy evolution of coal-rock combination under cyclic loading," *Shock and Vibration*, vol. 2020, pp. 1–16, 2020.

[29] S. Yang, J. Wang, J. Ning, and P. Qiu, "Experimental study on mechanical properties, failure behavior and energy evolution of different coal-rock combined specimens," *Applied Sciences*, vol. 9, no. 20, pp. 4427–4438, 2019.

[30] F. Q. Gong, H. Ye, and Y. Luo, "The effect of high loading rate on the behaviour and mechanical properties of coal-rock combined body," *Shock and Vibration*, vol. 2018, pp. 1–9, Article ID 4374530, 2018.

[31] J. Liu, E. Wang, D. Song, S. Wang, and Y. Niu, "Effect of rock strength on failure mode and mechanical behavior of composite samples," *Arabian Journal of Geosciences*, vol. 8, no. 7, pp. 4527–4539, 2014.

[32] G. Wu, W. Yu, J. Zuo, and S. du, "Experimental and theoretical investigation on mechanisms performance of the rock-coal-bolt (RCB) composite system," *International Journal of Mining Science and Technology*, vol. 30, no. 6, pp. 759–768, 2020.

[33] S. Chen, D. Yin, N. Jiang, F. Wang, and Z. Zhao, "Mechanical properties of oil shale-coal composite samples," *International Journal of Rock Mechanics and Mining Sciences*, vol. 123, Article ID 104120, 2019.

[34] Z. H. Chen, C. A. Tang, and R. Q. Huang, "A double rock sample model for rockbursts," *International journal of rock mechanics and mining sciences*, vol. 34, no. 6, pp. 991–1000, 1997.

[35] F. Gao, H. Kang, and L. Yang, "Experimental and numerical investigations on the failure processes and mechanisms of composite coal-rock specimens," *Scientific Reports*, vol. 10, no. 1, p. 13422, 2020.

[36] F. Gao and L. Yang, "Experimental and numerical investigation on the role of energy transition in strainbursts," *Rock Mechanics and Rock Engineering*, vol. 54, no. 9, pp. 5057–5070, 2021.

[37] L. Yang, F. Q. Gao, X. Q. Wang, and J. Z. Li, "Energy evolution law and failure mechanism of coal-rock combined specimen," *Journal of China Coal Society*, vol. 44, no. 12, pp. 3894–3902, 2019.

[38] Y.-L. Tan, W.-Y. Guo, and Q.-H. Gu, "Research on the rockburst tendency and AE characteristics of Inhomogeneous coal-rock combination bodies," *Shock and Vibration*, vol. 2016, p. 1, Article ID 9271434, 2016.

[39] Q. Ma, Y.-l. Tan, X.-s. Liu, Z.-h. Zhao, and D.-y. Fan, "Mechanical and energy characteristics of coal-rock composite sample with different height ratios: a numerical study based on particle flow code," *Environmental Earth Sciences*, vol. 80, no. 8, pp. 309–321, 2021.

[40] Q. Ma, Y. Tan, X. Liu, Q. Gu, and X. Li, "Effect of coal thicknesses on energy evolution characteristics of roof rock-coal-floor rock sandwich composite structure and its damage constitutive model," *Composites Part B: Engineering*, vol. 198, Article ID 108086, 2020.

[41] F. Du, K. Wang, X. Dong, and J. Wei, "Numerical simulation of damage and failure of coal-rock combination based on CT three-dimensional reconstruction," *Journal of China Coal Society*, vol. 1079, 2020.

[42] K. Wang, F. Du, X. Zhang, L. Wang, and C. Xin, "Mechanical properties and permeability evolution in gas-bearing coal-rock combination body under triaxial conditions," *Environmental Earth Sciences*, vol. 76, no. 24, p. 815, 2017.

[43] K. Wang and F. Du, "Experimental investigation on mechanical behavior and permeability evolution in coal-rock combined body under unloading conditions," *Arabian Journal of Geosciences*, vol. 12, no. 14, 2019.

[44] F. Du, K. Wang, G. Wang, Y. Jiang, C. Xin, and X. Zhang, "Investigation of the acoustic emission characteristics during deformation and failure of gas-bearing coal-rock combined bodies," *Journal of Loss Prevention in the Process Industries*, vol. 55, pp. 253–266, 2018.

[45] J. Lu, G. Yin, B. Deng et al., "Permeability characteristics of layered composite coal-rock under true triaxial stress conditions," *Journal of Natural Gas Science and Engineering*, vol. 66, pp. 60–76, 2019.

[46] J. Lu, G. Huang, H. Gao, X. Li, D. Zhang, and G. Yin, "Mechanical properties of layered composite coal-rock subjected to true triaxial stress," *Rock Mechanics and Rock Engineering*, vol. 53, no. 9, pp. 4117–4138, 2020.

[47] J. Lu, D. Zhang, G. Huang, X. Li, H. Gao, and G. Yin, "Effects of loading rate on the compound dynamic disaster in deep underground coal mine under true triaxial stress," *International Journal of Rock Mechanics and Mining Sciences*, vol. 134, Article ID 104453, 2020.

[48] X. S. Liu, Y. L. Tan, J. G. Ning, Y. W. Lu, and Q. H. Gu, "Mechanical properties and damage constitutive model of coal in coal-rock combined body," *International Journal of Rock Mechanics and Mining Sciences*, vol. 110, pp. 140–150, 2018.

[49] J. Zuo, Y. Chen, H. Song, and X. Wei, "Evolution of pre-peak axial crack strain and nonlinear model for coal-rock combined body," *Chinese Journal of Geotechnical Engineering*, vol. 39, no. 9, pp. 1609–1615, 2017.

[50] J. P. Zuo, H. Q. Song, Y. Chen, and Y. H. Li, "Post-peak progressive failure characteristics and nonlinear model of coal–rock combined body," *Journal of China Coal Society*, vol. 43, no. 12, pp. 3265–3272, 2018.

[51] H. Q. Song, J. P. Zuo, and Y. Chen, "Post–peak stress-strain relationship model and brittle characteristics of coal–rock combined body," *Journal of Mining and Safety Engineering*, vol. 35, pp. 1063–1070, 2018.

[52] I. M. Petukhov and A. M. Linkov, "The theory of post-failure deformations and the problem of stability in rock mechanics," *International Journal of Rock Mechanics and Mining Sciences & Geomechanics Abstracts*, vol. 16, no. 2, pp. 57–76, 1979.

[53] S. Q. Qin, J. J. Jiao, C. A. Tang, and Z. Li, "Instability leading to coal bumps and nonlinear evolutionary mechanisms for a coal-pillar-and-roof system," *International Journal of Solids and Structures*, vol. 43, no. 25-26, pp. 7407–7423, 2006.

[54] H. Xie, Z. Chen, and H. Zhou, "Study on two-body mechanical model based on interaction between structural body and geo-body," *Chinese Journal of Rock Mechanics and Engineering*, vol. 24, no. 9, pp. 1457–1464, 2005.

[55] X. B. Deng, H. J. Hu, G. Xu, X. T. Li, and F. Y. Chen, "Numerical simulation for burst failure of two-body rock structure," *Journal of Mining & Safety Engineering*, vol. 29, pp. 833–839, 2012.

[56] Z. Zhao, W. Wang, L. Wang, and C. Dai, "Compression-shear strength criterion of coal-rock combination model considering interface effect," *Tunnelling and Underground Space Technology*, vol. 47, no. 47, pp. 193–199, 2015.

[57] Z.-h. Zhao, W.-m. Wang, C.-q. Dai, and J.-x. Yan, "Failure characteristics of three-body model composed of rock and coal with different strength and stiffness," *Transactions of Nonferrous Metals Society of China*, vol. 24, no. 5, pp. 1538–1546, 2014.

[58] H. Song, J. Zuo, H. Liu, and S. Zuo, "The strength characteristics and progressive failure mechanism of soft rock-coal combination samples with consideration given to interface effects," *International Journal of Rock Mechanics and Mining Sciences*, vol. 138, Article ID 104593, 2021.

[59] K. Yang, W. J. Liu, L. T. Dou, X. L. Chi, Z. Wei, and Q. Fu, "Experimental investigation into interface effect and progressive instability of coal-rock combined specimen," *Journal of China Coal Society*, vol. 45, no. 5, pp. 1691–1700, 2020.